A POCS-Based Restoration Algorithm for Restoring Halftoned Color-Quantized Images

Yik-Hing Fung and Yuk-Hee Chan

***Abstract*—This paper studies the restoration of images which are color-quantized with error diffusion. Though there are many reported algorithms proposed for restoring noisy blurred color images and inverse halftoning, restoration of color-quantized images is rarely addressed in the literature especially when the images are color-quantized with halftoning. Direct application of existing restoration techniques are generally inadequate to deal with this problem. In this paper, a restoration algorithm based on projection onto convex sets is proposed. This algorithm makes use of the available color palette and the mechanism of a halftoning process to derive useful *a priori* information for restoration. Simulation results showed that it could improve the quality of a halftoned color-quantized image remarkably in terms of both SNR and CIELAB color difference metric.**

***Index Terms*—Color palette, color restoration, color quantization, error diffusion, image restoration, inverse halftoning, projection onto convex sets (POCS).**

I. INTRODUCTION

COLOR quantization is the process of reducing the number of colors in a digital image by replacing them with a representative color selected from a palette [1], [2]. This palette is usually image dependent. It can be of any arbitrary size and contain arbitrary colors. When color quantization is performed, certain types of degradation are introduced due to the limited colors used to produce the output image. Digital halftoning [3] would be helpful to eliminate these defects by making use of the fact that human eyes act as spatial low-pass filters. At the moment, the most popular halftoning method is error diffusion and several well-known error diffusion filters, such as the Floyd–Steinberg filter [4], Jarvis–Judice–Ninke filter [5], and Stucki filter [6] are generally used to achieve the goal. Fig. 1 shows the functional block diagram of a system which performs color quantization with error diffusion. Hereafter, we refer to the output of this system as a *halftoned color-quantized image*.

Color quantization is a kind of degradation to the original full-color image. Sometimes image restoration is necessary to recover the original image from its color-quantized version. This is especially true when the color-quantized version is required to be further processed or compressed. However, though there are a lot of reported works on the restoration of noisy and blurred color images, little effort has been seen in the literature for restoring halftoned color-quantized images. Obviously, the degradation models of the two cases are completely different and hence direct adoption of conventional restoration algorithms does not work effectively. Recently, a restoration algorithm for handling color-quantized images has been proposed, but it does not take account of the case when halftoning is involved in the quantization process [7].

Inverse halftoning can be used to restore binary halftones to its original [8]–[13]. In printing applications, color images are decomposed into three or four color components (CMY or CMYK). Each color plane is then considered as an individual gray scale image and they are separately halftoned with a conventional binary halftoning algorithm. In such cases, a straightforward extension of a conventional inverse halftoning algorithm can do the job as one can restore each color plane with an inverse halftoning algorithm directly. However, this straightforward approach only works for handling color halftones in which the colors are composed of a few of bi-level fixed color components.

Color quantization is actually a vector quantization instead of a bi-level uniform scalar quantization as in the case of binary halftoning. It is not a combination of several independent bi-level uniform scalar quantization processes either. In general, when a low-end display unit such as a VGA monitor is involved, the palette colors are not uniformly distributed in the color space. By considering this, restoring color halftones generated for printing applications is only a special case of the problem concerned in this paper. In particular, it is equivalent to the case that a palette $\{(C,M,Y)|C,M,Y=0,1\}$, where 0 and 1 denote the minimum and maximum intensity values respectively, is used in color quantization.

Fig. 2 shows how a color palette clusters a cross section of a color space. As shown in Fig. 2(a), in the restoration of color halftones generated for printing applications, one can easily define the bounds of a cluster in all dimensions and derive a simple constraint set for color restoration. However, in the general case with which we are tackling, since the involved palette can be of arbitrary size and contain arbitrary colors, clusters can be of arbitrary shape and size. Hence, it is not easy to precisely define their boundaries. Fig. 2(b) shows an example of this general case. The solid lines in Fig. 2(b) are the cluster boundaries which partition the cross section in this example.

Even though an inverse halftoning algorithm is extended to handle halftones involving multi-level quantization, processing color planes separately does not work effectively. It is because, due to the implicit assumptions that this approach has, one has to approximate the clusters with rectangular column in restoration. The dotted lines in Fig. 2(b) show the approximation result

Manuscript received August 20, 2004; revised August 9, 2005. This work was supported in part by the Research Grants Council of the Hong Kong Special Adminstrative Region, China, under Grant PolyU 5217/03E, and in part by the Centre for Multimedia Signal Processing, Hong Kong Polytechnic University. The associate editor coordinating the review of this manuscript and approving it for publication was Prof. Vincent Caselles.

The authors are with the Centre for Multimedia Signal Processing, Department of Electronic and Information Engineering, The Hong Kong Polytechnic University, Kowloon, Hong Kong, China (e-mail: enyhchan@polyu.edu.hk).

Digital Object Identifier 10.1109/TIP.2006.873432

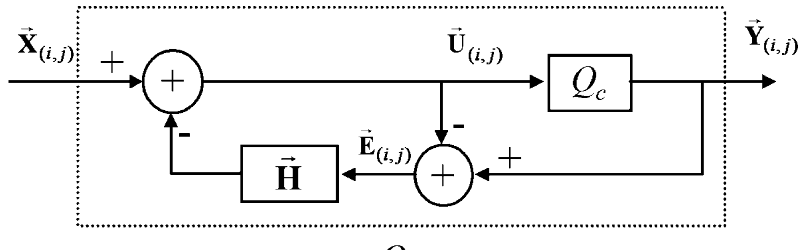

Fig. 1. Color quantization with error diffusion.

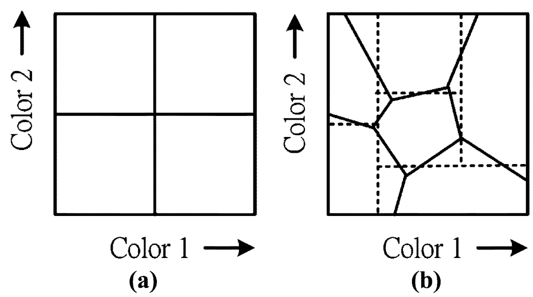

Fig. 2. How a cross section of a color space is partitioned by a color palette: (a) in a color halftone generated for printing applications and (b) in general color quantization.

of the presented example. One can see that the approximation error can be very large and hence processing color planes separately with inverse halftoning algorithms cannot provide a good restoration result in general. In other words, further extension of existing binary inverse halftoning algorithms for handling the general case is not as straightforward as most people assume.

This paper is devoted to formulating the process of color quantization in which error diffusion is involved and developing a POCS-based restoration algorithm to restore corresponding degraded images. The proposed restoration algorithm is able to restore any images which are color-quantized with an arbitrary color palette and an error diffusion process.

II. Image Degradation in Color Quantization With Error Diffusion

A 24-bit full-color image $\mathbf{X}$ generally consists of three 8-bit color planes, say, $\mathbf{X_r}$, $\mathbf{X_g}$, and $\mathbf{X_b}$, which represents the red, the green, and the blue color planes of the image, respectively. A pixel is then a vector represented as $\vec{\mathbf{X}}_{(i,j)} = (\mathbf{X}_{(i,j)r}, \mathbf{X}_{(i,j)g}, \mathbf{X}_{(i,j)b})$, where $\mathbf{X}_{(i,j)c} \in [0,1]$ is the intensity value of the cth color component of the (i,j)th pixel. Here, we assume that the image is of size $N \times N$ and the maximum and the minimum intensity values of a pixel are, respectively, 1 and 0.

Fig. 1 shows the system which performs color quantization with error diffusion. The input image $\mathbf{X}$ is scanned in a row-by-row fashion from pixel (1,1) to pixel (N,N) and processed as follows to produce the encoded image $\mathbf{Y}$

$$\mathbf{U}_{(i,j)c} = \mathbf{X}_{(i,j)c} - \sum_{(k,l)\in S} \mathbf{H}_{(k,l)c}\mathbf{E}_{(i-k,j-l)c} \quad (1)$$

$$\vec{\mathbf{Y}}_{(i,j)} = Q_c[\vec{\mathbf{U}}_{(i,j)}] \quad (2)$$

$$\text{and } \vec{\mathbf{E}}_{(i,j)} = \vec{\mathbf{Y}}_{(i,j)} - \vec{\mathbf{U}}_{(i,j)} = Q_c[\vec{\mathbf{U}}_{(i,j)}] - \vec{\mathbf{U}}_{(i,j)} \quad (3)$$

where $\vec{\mathbf{U}}_{(i,j)}$ is a state vector of the system, $\vec{\mathbf{E}}_{(i,j)}$ is the quantization error of the pixel at position (i,j) and $\mathbf{H}_{(k,l)c}$ is a coefficient of the error diffusion filter for the cth color component. S is the casual support region of $\mathbf{H}_{(k,l)c}$.

The operator $Q_c[\bullet]$ performs a 3-D vector quantization. Specifically, the 3-D vector $\vec{\mathbf{U}}_{(i,j)}$ is compared with a set of representative color vectors stored in a previously generated color palette $C = \{\hat{\mathbf{v}}_i : i = 1, 2, \ldots N_c\}$. The best-matched vector in the palette is selected based on the minimum Euclidean distance criterion. In other words, a state vector $\vec{\mathbf{U}}_{(i,j)}$ is represented by color $\hat{\mathbf{v}}_k$ if and only if $\|\vec{\mathbf{U}}_{(i,j)} - \hat{\mathbf{v}}_k\| \le \|\vec{\mathbf{U}}_{(i,j)} - \hat{\mathbf{v}}_l\|$ for all $l = 1, 2 \ldots N_c$. Once the best-matched vector is selected from the color palette, its index is recorded and the quantization error $\vec{\mathbf{E}}_{(i,j)} = \hat{\mathbf{v}}_k - \vec{\mathbf{U}}_{(i,j)}$ is diffused to pixel (i,j)'s neighborhood with (1). To handle the boundary pixels, $\vec{\mathbf{E}}_{(i,j)}$ is defined to be zero when (i,j) falls outside the image.

After the scanning is finished, the recorded indexes can be used in the future to reconstruct the color-quantized image with the same color palette.

III. *A Priori* Information

The proposed algorithm is a POCS-based algorithm which makes an estimation of the original image $\mathbf{X}$ with the observed $\mathbf{Y}$ by projecting intermediate estimates among convex constraint sets iteratively. The constraint sets used in the algorithm are formulated in this section.

Suppose we have already made an estimation of $\mathbf{X}$ to get an intermediate estimate $\mathbf{X}'$ and are going to refine our estimate. The pixels of $\mathbf{X}'$ are adjusted one by one in the refinement. The order in that the pixels are adjusted follows the order in that the pixels were color-quantized. Here, we assume that the degradation process Q_{ch} is known.

Without loss of generality, consider we are now processing pixel (m,n). As we have mentioned, pixels are adjusted one by one as they were processed in color quantization. All previously adjusted pixels and pixel (m,n) of $\mathbf{X}'$ form a partial image and can be color-quantized with operation Q_{ch} (1)–(3) until pixel (m,n) is reached. For the sake of reference, this partial image is referred to as $\mathbf{I}_p$ and the set of the coordinates of the adjusted pixels and (m,n) is referred to as Ω_p hereafter. When $\mathbf{I}_p$ is color-quantized with (1)–(3), intermediate state vectors $\vec{\mathbf{U}}_{(k,l)}$ and error vectors $\vec{\mathbf{E}}_{(k,l)}$, where $(k,l) \in \Omega_p$, are generated. They are referred to as $\vec{\mathbf{U}}'_{(k,l)}$ and $\vec{\mathbf{E}}'_{(k,l)}$.

Obviously, since the observed image $\mathbf{Y}$ is the color-quantized output of the original image $\mathbf{X}$, the color-quantized output of our estimate of $\mathbf{X}$ should also be $\mathbf{Y}$. In other words, we should

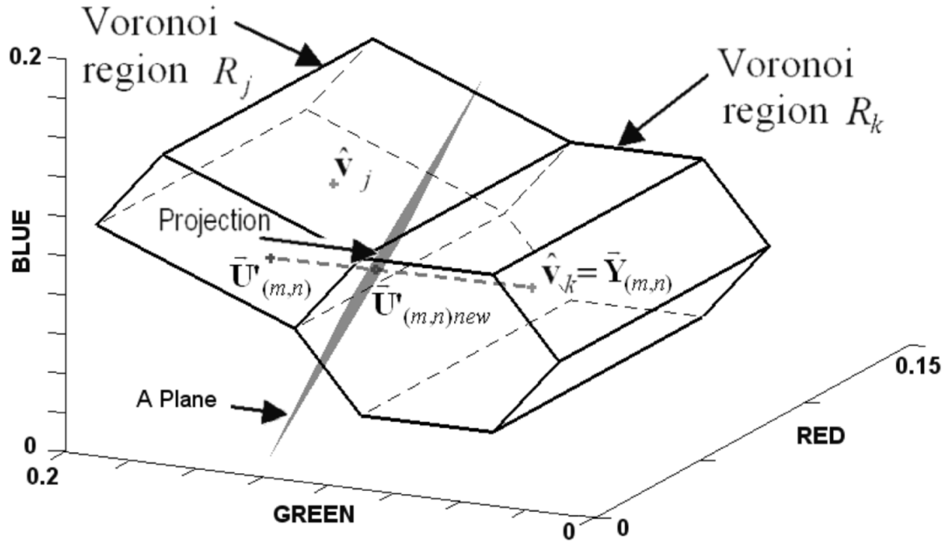

Fig. 3. Projection of $\vec{\mathbf{U}}'_{(m,n)}$ onto R'_k.

have $Q_{ch}[\vec{\mathbf{X}}'_{(m,n)}] = \vec{\mathbf{Y}}_{(m,n)}$, where $Q_{ch}[\vec{\mathbf{I}}_{(m,n)}]$ denotes the (m,n)th pixel of the output when image $\mathbf{I}$ is processed with (1)–(3) from pixel (1,1) to pixel (m,n). Accordingly, after adjusting pixel (m,n), a convex constraint set in which the desirable output image should be can be formed as follows:

$$S_{2,(m,n)}\left\{\mathbf{I} \mid \vec{\mathbf{I}}_{(i,j)} = \vec{\mathbf{X}}''_{(i,j)} \ \forall\,(i,j) \in \Omega_p \backslash (m,n) \right. \\ \vec{\mathbf{I}}_{(i,j)} = \vec{\mathbf{X}}'_{(i,j)} \ \forall\,(i,j) \notin \Omega_p \text{ and} \\ \left. Q_{ch}[\vec{\mathbf{I}}_{(m,n)}] = \vec{\mathbf{Y}}_{(m,n)} \right\} \tag{4}$$

where $\vec{\mathbf{X}}''_{(i,j)}$ is the adjusted $\vec{\mathbf{X}}'_{(i,j)}$ in the refinement and $\mathbf{I}$ is an image whose size is the same as $\mathbf{X}$.

Recall that $\vec{\mathbf{X}}'_{(m,n)}$ is the estimate of $\vec{\mathbf{X}}_{(m,n)}$ before adjustment. If $Q_{ch}[\vec{\mathbf{X}}'_{(m,n)}] = \vec{\mathbf{Y}}_{(m,n)}$ happens, the current state of the refined $\mathbf{X}'$ will be a member of $S_{2,(m,n)}$ and no adjustment of $\vec{\mathbf{X}}'_{(m,n)}$ will be required. However, it is possible that $Q_{ch}[\vec{\mathbf{X}}'_{(m,n)}] \neq \vec{\mathbf{Y}}_{(m,n)}$ as the $\vec{\mathbf{U}}'_{(m,n)}$ obtained with (1) is out of R_k as shown in Fig. 3. Here, R_k is defined as the Voronoi region associated with palette color $\hat{\mathbf{v}}_k (= \vec{\mathbf{Y}}_{(m,n)})$. In other words, we have $Q_c[\vec{\mathbf{U}}'_{(m,n)}] \neq \vec{\mathbf{Y}}_{(m,n)}$ in formulation. In such a case, a projection is necessary to project $\vec{\mathbf{U}}'_{(m,n)}$ onto the boundary of R_k.

The projection is carried out as follows. Starting from $\vec{\mathbf{U}}'_{(m,n)}$, we search along the straight line connecting $\vec{\mathbf{U}}'_{(m,n)}$ and $\vec{\mathbf{Y}}_{(m,n)}$ to seek a new point $\vec{\mathbf{U}}'_{(m,n)\text{new}}$ such that $Q_c[\vec{\mathbf{U}}'_{(m,n)\text{new}}] = \vec{\mathbf{Y}}_{(m,n)}$ is satisfied. The search is conducted with estimates generated iteratively with

$$\vec{\mathbf{U}}'_{(m,n)\text{new}} = \vec{\mathbf{Y}}_{(m,n)} + \lambda^n (\vec{\mathbf{U}}'_{(m,n)} - \vec{\mathbf{Y}}_{(m,n)}) \tag{5}$$

where λ^n is a relaxation parameter at iteration n. The convergence of the estimate can be guaranteed as long as $0 \leq \lambda < 1$. After $\vec{\mathbf{U}}'_{(m,n)\text{new}}$ is found, $\vec{\mathbf{U}}'_{(m,n)}$ is updated to be $\vec{\mathbf{U}}'_{(m,n)\text{new}}$.

Note that this point-to-point projection may not be perpendicular to the surface of R_k. However, this does not matter. As shown in Fig. 3, one can define a plane which passes $\vec{\mathbf{U}}'_{(m,n)\text{new}}$ and is perpendicular to the line connecting $\vec{\mathbf{U}}'_{(m,n)}$ and $\vec{\mathbf{Y}}_{(m,n)}$. In formulation, the equation of the plane is given as

$$\left(\vec{\mathbf{p}} - \vec{\mathbf{U}}'_{(m,n)\text{new}}\right) \bullet \left(\vec{\mathbf{U}}'_{(m,n)} - \vec{\mathbf{Y}}_{(m,n)}\right) = 0 \tag{6}$$

where $\vec{\mathbf{p}} \in R_k$ is a pixel vector in the color space and $\bullet$ denotes the dot product operator of two vectors. This plane cuts through Voronoi region R_k and splits it into two. The one containing point $\vec{\mathbf{Y}}_{(m,n)}$ forms a new constraint set R'_k. By doing so, projection from $\vec{\mathbf{U}}'_{(m,n)}$ to $\vec{\mathbf{U}}'_{(m,n)\text{new}}$ is equivalent to a projection onto a convex set R'_k.

After determining $\vec{\mathbf{U}}'_{(m,n)}$, the adjusted $\vec{\mathbf{X}}'_{(m,n)}$ can be obtained by

$$\mathbf{X}''_{(m,n)c} = \mathbf{U}'_{(m,n)c} + \sum_{(k,l)\in S} \mathbf{H}_{(k,l)c}\mathbf{E}'_{(m-k,n-l)c} \\ \text{for } c \in \{r,g,b\}. \tag{7}$$

The adjusted image is then a member of $S_{2,(m,n)}$. The constraint set $S_{2,(m,n)}$ and its associated projection presented above is dedicated for handling halftoned color-quantized images with POCS.

Fig. 4 shows two examples of how the pixels of the current estimate $\mathbf{X}'$ are handled during the adjustment. Without loss of generality, in these examples, we assume gray-level images and use a two-color palette to make the examples simple enough to illustrate the approach clearly. Pixels (2,2) and (2,3) are, respectively, the pixels being handled in the first and the second examples. The shaded positions mark the pixels that were handled at the moment. In the first example, $\vec{\mathbf{U}}'_{(2,2)}$ is determined with (1). Since we have $Q_c[\vec{\mathbf{U}}'_{(2,2)}] = \vec{\mathbf{Y}}_{(2,2)} = (0.2, 0.2, 0.2)$, no adjustment of $\vec{\mathbf{X}}'_{(2,2)}$ is required. $\vec{\mathbf{E}}'_{(2,2)}$ is updated with (3) then. In the second example, we have $Q_c[\vec{\mathbf{U}}'_{(2,3)}] \neq \vec{\mathbf{Y}}_{(2,3)}$. Adjustment of $\vec{\mathbf{X}}'_{(2,3)}$ is hence necessary. The adjustment is carried out by iteratively adjusting $\vec{\mathbf{U}}'_{(2,3)}$ with (5). At iteration $n = 3$, $\vec{\mathbf{U}}'_{(2,3)}$ is adjusted to be (0.51, 0.51, 0.51), which makes $Q_c[\vec{\mathbf{U}}'_{(2,3)}] = \vec{\mathbf{Y}}_{(2,3)} = (0.8, 0.8, 0.8)$. The corresponding $\vec{\mathbf{X}}'_{(2,3)}$ and $\vec{\mathbf{E}}'_{(2,3)}$ can then be obtained with (7) and (3), respectively.

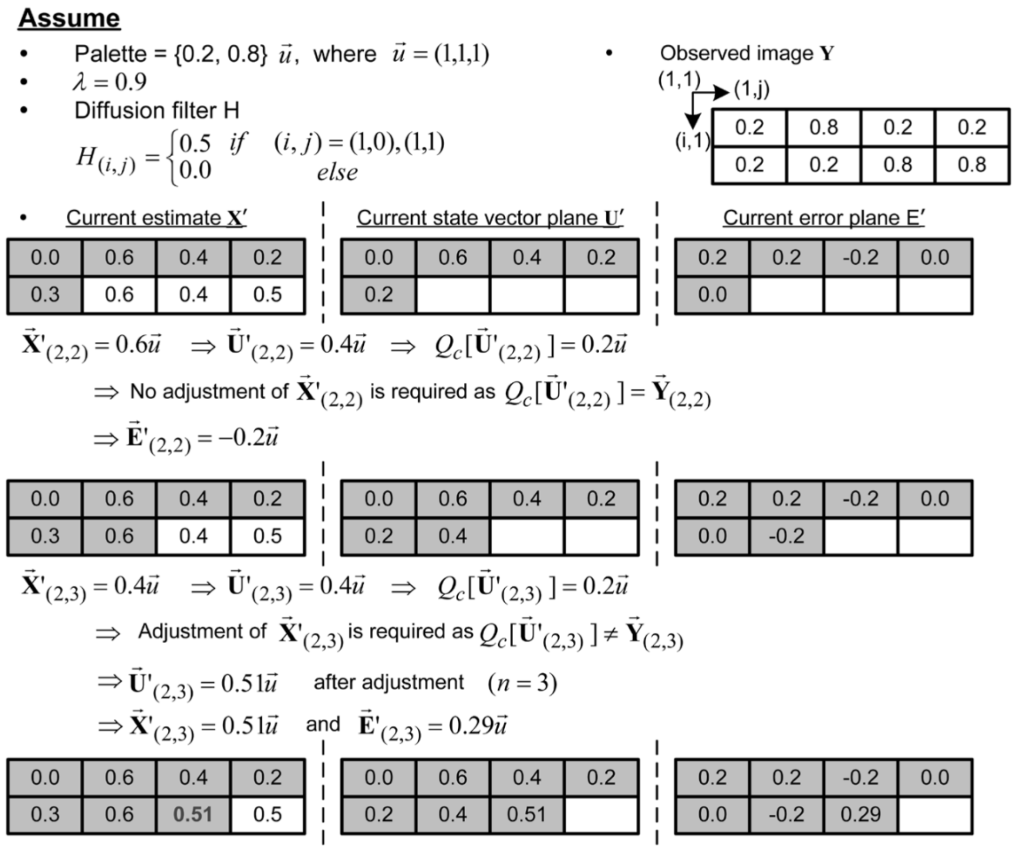

Fig. 4. Examples of how pixels of an estimate of the original image are updated.

Typical images would generally have weak high frequency components as the intensity of neighboring pixels is highly correlated. This feature can be exploited as *a priori* information in the restoration of halftoned color-quantized images. In our approach, we assume that the energy of each high frequency component of $\mathbf{X}$ is bounded as given by $|[T(\mathbf{X})]_{(u,w)}| \leq |[T(F(\mathbf{Y}))]_{(u,w)}|$ for $(u,w) \in \Omega_H$, where F and T are, respectively, a linear low-pass filtering operator and a 2-D DCT operator, $[\bullet]_{(u,w)}$ denotes the (u,w)th element in the transform domain and Ω_H defines the set of high frequency components which should be bounded. This forms a smoothness constraint set

$$S_1 = \left\{ \mathbf{I} \mid |[T(\mathbf{X})]_{(u,w)}| \leq |[T(F(\mathbf{Y}))]_{(u,w)}| \right. \\ \left. \text{for } (u,w) \in \Omega_H \right\}. \quad (8)$$

Another constraint set for restoring $\mathbf{X}$ is the one that confines the intensity value of a particular pixel to be valid. In formulation, we have

$$S_3 = \{\mathbf{I} \mid \vec{\mathbf{I}}_{(i,j)} \in \Gamma, \ \forall\, (i,j)\} \quad (9)$$

where $\Gamma = \{(r,g,b) \mid 0 \leq r,g,b \leq 1\}$.

IV. Formulation of POCS Algorithm

A POCS-based iterative algorithm can be defined based on the convex constraint sets defined in the previous section. In formulation, we have

$$\mathbf{X}^{(m+1)} = P_3 P_{2,(N,N)} \ldots P_{2,(i,j)} \ldots P_{2,(1,1)} P_1 \mathbf{X}^{(m)} \quad (10)$$

where $\mathbf{X}^{(m)}$ is the estimate of $\mathbf{X}$ at iteration m, P_1, $P_{2,(i,j)}$, and P_3 are the projection operators to project a given image $\mathbf{I}$ onto S_1, $S_{2,(i,j)}$, and S_3, respectively. In particular, P_1 and $P_{2,(i,j)}$ are defined as shown in (11)–(12), at the bottom of the next page, where $\beta_{(i,j)}$ is the corresponding λ^n for pixel (i,j) to adjust $\vec{\mathbf{U}}'_{(i,j)}$ with (5) such that $Q_c[\vec{\mathbf{U}}'_{(i,j)}] = \vec{\mathbf{Y}}_{(i,j)}$ can be satisfied, and P_3 is defined as follows:

$$P_3 : \mathbf{I}_{(i,j)c} = \begin{cases} 1, & \text{if } \mathbf{I}_{(i,j)c} > 1 \\ 0, & \text{if } \mathbf{I}_{(i,j)c} < 0 \end{cases} \\ \text{for } c \in \{r,g,b\}, \quad \forall\, (i,j). \quad (13)$$

Note that the pixels of the image were processed one by one from position (1,1) to (N,N) in a raster scanning order when projections $P_{2,(i,j)}$s are performed. This order corresponds to the order that the pixels were processed during its color quantization. The examples shown in Fig. 4 correspond to projections $P_{2,(2,2)}$ and $P_{2,(2,3)}$. The initial estimate $\mathbf{X}^{(0)}$ is set to be $F(\mathbf{Y})$ which is a filtered version of the observed image. Since all involved constraint sets are convex sets, the convergence of POCS algorithm can be guaranteed.

The physical meaning of the projections is as follows. Projection P_1 guarantees that the energy of the high frequency components of the restored image is less than the energy of the high frequency components of the low-pass filtering result of the observed image. Projection $P_{2,(i,j)}$ makes sure that the color-quantized result of the restored image is exactly the same as the observed image from the first processing pixel to the (i,j)th pixel. With the use of projection P_3, all pixels of the restored image are displayable.

In this paper, the proposed algorithm is formulated in RGB color space. This is based on the observation that a palette for a video color display is usually defined in RGB domain. With an approach similar to the one presented in this paper, the proposed algorithm can be reformulated in other color spaces.

V. Simulation and Comparative Study

Simulation was carried out to evaluate the performance of the proposed algorithm. In our simulation, a number of *de facto* standard 24-bit full-color images including *Couple*, *Window*, *Peppers*, *Fruits*, *Lena*, *House*, *Girl*, *Parrots*, *Pool*, *Caps*, *Baboon*, and *Melon* were used. Each of them is of size 256×256. The images were color-quantized to produce $\mathbf{Y}$s. Color palettes of different size were used in color quantization and they were generated with different palette generation algorithms. In color quantization, halftoning was performed with error diffusion and Floyd–Steinberg diffusion filter [4] was used. In the realization of the proposed algorithm, a 3×3 Gaussian filter was used as filter F. Ω_H and λ were, respectively, selected to be $\{(u,w)|(256-u)^2+(256-w)^2 < 100\,000$ and $0 \le u, w < 256\}$ and 0.9.

To our best knowledge, there is no reported restoration algorithm directly proposed for restoring halftoned color-quantized images [14]. Fung's algorithm [7] was proposed for restoring color-quantized images, but it assumes that there is no halftoning involved in color quantization. Mese's algorithm [8] was originally proposed for inverse halftoning. It makes use of some training images to pre-train a linear prediction filter for filtering binary halftones. For comparison, it was modified here to handle halftoned color-quantized images.

Mese's algorithm trains a linear prediction filter with best linear estimator [8]. In the training phase, *Baboon*, *Melon*, *House*, *Lenna* and their corresponding halftoned color-quantized images were used to train the filter. As for Fung's algorithm [7] and the proposed algorithm, no original full-color image is required to extract information and no training images are required to pre-train a linear prediction filter.

Table I shows the average restoration performance of different algorithms in terms of Signal-to-noise Ratio Improvement (SNRI) and CIELAB color difference (ΔE) metric. The involved palettes were obtained with median-cut algorithm [2]. The CIELAB color difference (ΔE) metric is defined as the Euclidean distance between the original color of a pixel and its reproduction in CIELAB color metric space [15]. It is well accepted that color error is visually detectable when $(\Delta E) > 3$ [16]. The figures in the tables are the average values obtained with the restoration results of the halftoned color-quantized images. One can see that the proposed algorithm is superior to the others. Fig. 5 shows the restoration results of different algorithms for visual evaluation. The high-frequency noise introduced by halftoning is greatly removed by the proposed algorithm. For example, impulse pattern noise can be found in the grapes and the pear in Fig. 5(c) and (d) while they are completely removed in Fig. 5(e). Besides, the sharp impulse noise in the mango is also significantly improved in Fig. 5(e). Similar results were obtained when the halftoned color-quantized images were produced with different palettes generated with different palette generation algorithms.

In the proposed algorithm, we assumed that the error diffusion filter used in color quantization is known in restoration. Sometimes this information may not be available and one has to estimate it from the observed images. The robustness of the proposed algorithm was studied. The last two columns of Table I show the simulation results obtained when different error diffusion filters were exploited in the realization of our proposed algorithm. Note that the three error diffusion filters [4]–[6] involved in the study are all popular filters used in practice. It was found that a wrong assumption resulted in less than 1 dB drop in SNRI on average. Even so, the proposed algorithm is still superior to the others.

As we have mentioned, restoring color halftones generated for printing applications is only a special case of the problem we concern. Existing inverse halftoning algorithms [8]–[12] can be easily extended to handle this case by restoring each color plane independently. Among them, Hein's algorithm [9] and Wong's algorithm [10] are POCS-based approaches in which different constraint sets are defined for inverse halftoning. Chang's algorithm [11] trains a MMSE lookup table to speed up the inverse halftoning process. When a nonexisting input is encountered in table lookup, LMS estimation is exploited. Kite's algorithm [12] is a spatially-varying linear filtering approach in which filter coefficients are data dependent and computed on the fly.

Simulations were carried out to compare their performance with ours in restoring this type of color halftones. Though Mese's algorithm [13] was originally proposed for restoring halftones produced with a special dot diffusion technique, it was also included in our simulation after a modification due to its POCS-based nature. Table II shows the simulation results. In our simulation, a color halftone was generated by halftoning each color plane of an original 24-bit full-color image to a bi-level image with error diffusion [4] and then combining all binary color planes together. Again, the same set of aforementioned testing images were used for evaluation. *Baboon*, *Melon*, *House*, *Lena*, and their corresponding halftoned color-quantized images were used in the training phase of Mese's [8] and Chang's [11] algorithms. Simulation results show that the proposed algorithm outperforms the others in various aspects. Besides the fact that the proposed algorithm makes a better use

$$P_1 : [T(\mathbf{I})]_{(u,w)} = [T(F(\mathbf{Y}))]_{(u,w)}, \text{ if } |[T(\mathbf{I})]_{(u,w)}| > |[T(F(\mathbf{Y}))]_{(u,w)}| \text{ for } (u,w) \in \Omega_H \tag{11}$$

$$P_{2,(i,j)} : \mathbf{I}_{(i,j)c} = \begin{cases} \mathbf{I}_{(i,j)c}, & \text{if } Q_c[\vec{\mathbf{U}}'_{(i,j)}] = \vec{\mathbf{Y}}_{(i,j)} \\ \mathbf{Y}_{(i,j)c} + \beta_{(i,j)}(\mathbf{U}'_{(i,j)c} - \mathbf{Y}_{(i,j)c}) + \sum\limits_{(k,l)\in S} \mathbf{H}_{(k,l)c}\mathbf{E}'_{(i-k,j-l)c}, & \text{if } Q_c[\vec{\mathbf{U}}'_{(i,j)}] \neq \vec{\mathbf{Y}}_{(i,j)} \end{cases}$$
$$\text{for } c \in \{r,g,b\} \quad \forall\, (i,j) \tag{12}$$

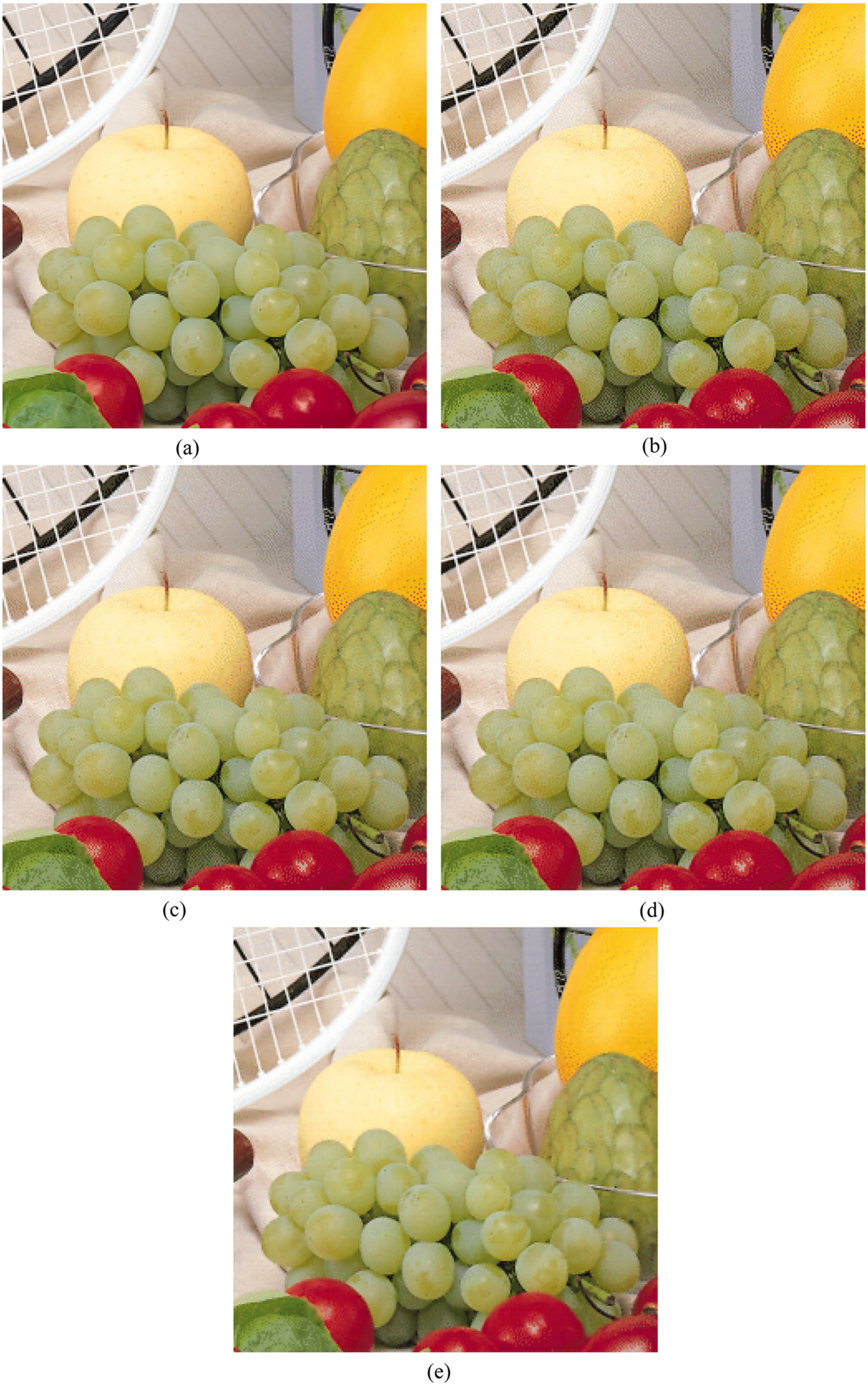

Fig. 5. Restoration results of color-quantized "Fruits" (Palette size $= 128$). (a) Original. (b) Color-quantized (with halftoning). (c) Fung [7]. (d) Mese [8]. (e) Proposed. (Color version available online at http://ieeexplore.ieee.org.)

TABLE I
AVERAGE PERFORMANCE OF VARIOUS ALGORITHMS IN RESTORING HALFTONED COLOR-QUANTIZED IMAGES IN VARIOUS ASPECTS

Palette size	Observed ($\mathbf{Y}$)	Restored ($\mathbf{X'}$)				
		Fung [7]	Mese [8]	Proposed	Proposed [1]	Proposed [2]
	Average of (SNR Improvement (dB))					
256	-	4.543	3.946	7.258	6.621	6.750
128	-	4.687	5.293	8.426	7.716	7.850
64	-	4.512	6.628	9.847	9.022	9.159
32	-	3.904	7.705	10.058	9.142	9.269
	Average of (Average of CIELAB difference ΔE)					
256	4.876	3.406	3.945	2.615	2.703	2.686
128	5.821	4.184	4.404	3.099	3.206	3.185
64	7.285	5.418	5.169	3.730	3.870	3.843
32	8.951	7.031	6.268	4.979	5.154	5.125
	Average of (% of pixels whose CIELAB $\Delta E < 3$)					
256	42.044	58.664	51.430	70.220	68.908	69.187
128	32.286	48.864	45.020	63.899	62.304	62.570
64	24.169	36.989	37.685	56.583	54.371	54.729
32	15.247	25.659	28.894	44.498	42.295	42.637

Observed $\mathbf{Y}$ is color-quantized with a palette generated with median-cut algorithm[2] and a Floyd-Steinberg filter[4].
[1]With a wrong assumption that Jarvis-Judice-Ninke diffusion filter [5] was used to produce $\mathbf{Y}$
[2]With a wrong assumption that Stucki diffusion filter [6] was used to produce $\mathbf{Y}$

TABLE II
AVERAGE PERFORMANCE OF VARIOUS INVERSE HALFTONING ALGORITHMS IN RESTORING COLOR HALFTONES

Palette size	Observed ($\mathbf{Y}$)	Restored ($\mathbf{X'}$)						
		Proposed	Mese [8]	Hein [9]	Wong [10]	Chang [11]	Kite [12]	Mese [13]
	Average of (SNR Improvement (dB))							
8	-	42.519	38.001	40.250	40.158	36.844	37.941	39.968
	Average of (Average of CIELAB difference ΔE)							
8	76.444	10.677	11.813	12.236	10.996	11.905	10.684	11.690
	Average of (% of pixels whose CIELAB $\Delta E < 3$)							
8	0.384	11.351	7.443	7.758	12.931	7.453	4.023	9.655

Color halftones $\mathbf{Y}$ were generated by halftoning each color plane of original color images individually with error diffusion.

of the available *a priori* information as compared with the other evaluated algorithms [8]–[13] in restoration, the superiority of the proposed algorithm over the algorithms [8]–[13] is partially due to the fact that these algorithms treat a color image as three independent color planes in the restoration while the proposed algorithm is not.

VI. CONCLUSION

So far, very little research has been carried out to address the restoration of halftoned color-quantized images. Although there are many restoration algorithms for restoring blurred and noisy color images and inverse halftoning, they are generally not adequate to handle halftoned color-quantized images. The noise introduced by color quantization with halftoning is basically signal dependent and is not white, which violates the assumptions adopted in most current multichannel restoration algorithms. Though Fung's algorithm [7] was proposed to restore color-quantized images, it does not take halftoning into account and hence cannot handle the case well either.

In this paper, we proposed a dedicated restoration algorithm for restoring halftoned color-quantized images. This algorithm makes use of the available color palette and the *a priori* knowledge about the halftoning process to derive useful information for restoration. Unlike some other conventional restoration algorithms, it requires no estimation of parameters describing the nature of the original full-color image and no training image to pre-train prediction filters. Simulation results demonstrated that the proposed algorithm can achieve a remarkable improvement in the quality of a halftoned color-quantized image in terms of both SNR and CIELAB color difference ΔE metric irrespective of the size and the production of the color palette exploited in the color quantization.

REFERENCES

[1] M. T. Orchard and C. A. Bouman, "Color quantization of images," *IEEE Trans. Signal Process.*, vol. 39, no. 12, pp. 2677–2690, Dec. 1991.

[2] P. Heckbert, "Color image quantization for frame buffer displays," *Comput. Graph.*, vol. 16, no. 4, pp. 297–307, 1982.

[3] R. S. Gentile, E. Walowit, and J. P. Allebach, "Quantization and multilevel halftoning of color images for near original image quality," *Proc. SPIE*, vol. 1249, pp. 249–259, 1990.

[4] R. W. Floyd and L. Steinberg, "An adaptive algorithm for spatial grayscale," *Proc. Soc. Inf. Display*, vol. 17, no. 2, pp. 75–77, 1976.

[5] J. F. Jarvis, C. N. Judice, and W. H. Ninke, "A survey of techniques for the display of continuous tone pictures on bi-level displays," *Comput. Graph. Image Process.*, vol. 5, pp. 13–40, 1976.

[6] P. Stucki, "MECCA—A Multiple Error Correcting Computation Algorithm for Bi-Level Image Hard Copy Reproduction," IBM Research Laboratory, Zurich, Switzerland, Tech. Rep. RZ1060, 1981.

[7] Y. H. Fung and Y. H. Chan, "POCS-Based algorithm for restoring color-quantised images," *Proc. Inst. Elect. Eng.*, vol. 151, no. 2, pp. 119–127, Apr. 2004.

[8] M. Mese and P. P. Vaidyanathan, "Look-Up table (LUT) method for inverse halftoning," *IEEE Trans. Image Process.*, vol. 10, no. 10, pp. 1566–1578, Oct. 2001.

[9] S. Hein and A. Zakhor, "Halftone to continuous-tone conversion of error-diffusion coded images," *IEEE Trans. Image Process.*, vol. 4, no. 2, pp. 208–216, Feb. 1995.

[10] P. Wong, "Inverse halftoning and kernel estimation for error diffusion," *IEEE Trans. Image Process.*, vol. 6, no. 4, pp. 486–498, Apr. 1995.

[11] P. C. Chang, C. S. Yu, and T. H. Lee, "Hybrid LMS-MMSE inverse halftoning technique," *IEEE Trans. Image Process.*, vol. 10, no. 1, pp. 95–103, Jan. 2001.

[12] T. D. Kite, N. Damera-Venkata, B. L. Evans, and A. C. Bovik, "A fast, high-quality inverse halftoning algorithm for error diffused halftones," *IEEE Trans. Image Process.*, vol. 9, no. 9, pp. 1583–1592, Sep. 2000.

[13] M. Mese and P. P. Vaidyanathan, "A mathematical description of the dot diffusion algorithm in image halftoning, with application in inverse halftoning," in *Proc. ICASSP*, Phoenix, AZ, 1999, pp. 3437–3440.

[14] Y. H. Fung and Y. H. Chan, "Restoration of halftoned color-quantized images using linear estimator," presented at the IEEE ICME, Toronto, ON, Canada, Jul. 9–12, 2006.

[15] C.I.E. (1978) Recommendations on Uniform Color Spaces, Color Difference Equations, Psychometric Color Terms, Suppl. 2 to CIE pub. 15 (E.-1.3.1) 1971/(TC-1.3.).

[16] C. Connolly, T. W. W. Leung, and J. Nobbs, "Colour measurement by video camera," *JSDC*, vol. 111, pp. 373–375, 1995.

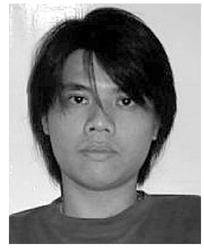

Yik-Hing Fung received the B.Eng. (Hons.) degree in 2000 from the Hong Kong Polytechnic University (HKPU), Kowloon, Hong Kong, China, where he is currently pursing the Ph.D. degree.

From 2000 to 2001, he was an Engineer with HKPU for a project entitled Web Based Portable Monitoring and Surveillance System. His research interests include image restoration, digital image halftoning, and image compression.

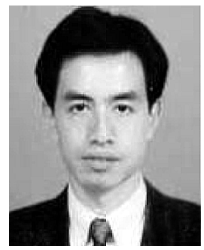

Yuk-Hee Chan received the B.Sc. degree with honors in electronics from Chinese University of Hong Kong in 1987, and the Ph.D. degree in signal processing from Hong Kong Polytechnic University in 1992.

Between 1987 and 1989, he was an R&D Engineer with Elec & Eltek Group, Hong Kong. He joined The Hong Kong Polytechnic University, Kowloon, in 1992 and is now an Associate Professor in the Department of Electronic and Information Engineering. He has published over 100 research papers in various international journals and conferences. His research interests include image and video compression, image restoration, and fast computational algorithms in DSP.

Dr. Chan is a member of the Institution of Electrical Engineers.